Pharm Res (2012) 29:603–617
DOI 10.1007/s11095-011-0607-2

RESEARCH PAPER

Novel *In Vitro-In Vivo* Extrapolation (IVIVE) Method to Predict Hepatic Organ Clearance in Rat

Ken-ichi Umehara • Gian Camenisch

Received: 3 December 2010 / Accepted: 10 October 2011 / Published online: 20 October 2011

ABSTRACT

Purpose Drug elimination in the liver consists of uptake, metabolism, biliary excretion, and sinusoidal efflux from the hepatocytes to the blood. We aimed to establish an accurate prediction method for liver clearance in rats, considering these four elimination processes. *In vitro* assays were combined to achieve improved predictions.

Methods *In vitro* clearances for uptake, metabolism, biliary excretion and sinusoidal efflux were determined for 13 selected compounds with various physicochemical and pharmacokinetic properties. Suspended hepatocytes, liver microsomes and sandwich-cultured hepatocytes were evaluated as *in vitro* models. Based on the individual processes, *in vivo* hepatic clearance was calculated. Subsequently, the predicted clearances were compared with the corresponding *in vivo* values from literature.

Results Using this *in vitro-in vivo* extrapolation method good linear correlation was observed between predicted and reported clearances. Linear regression analysis revealed much improved prediction for the novel method ($r^2 = 0.928$) as compared to parameter analysis using hepatocyte uptake only ($r^2 = 0.600$), microsomal metabolism only ($r^2 = 0.687$) or overall hepatobiliary excretion in sandwich-cultured hepatocytes ($r^2 = 0.321$).

Conclusions In this new attempt to predict hepatic elimination under consideration of multiple clearance processes, *in vivo* hepatic clearances of 13 compounds in rats were well predicted using an IVIVE analysis method based on *in vitro* assays.

K.-i. Umehara (✉) • G. Camenisch
Drug-Drug Interaction Section (DDI)
Drug Metabolism and Pharmacokinetics (DMPK)
Novartis Institutes of Biomedical Research (NIBR)
Novartis Pharma AG, WSJ-153.2.02., Novartis Campus
CH-4002, Basel, Switzerland
e-mail: ken-ichi.umehara@novartis.com

KEY WORDS biliary excretion · hepatic uptake · prediction · sinusoidal efflux · suspended and sandwich-cultured hepatocytes

ABBREVIATIONS

A	total intracellular amount of radioactivity in sandwich-cultured hepatocytes
ABC	ATP binding cassette
ATP	adenosintriphosphate
BCRP	breast cancer resistance protein
BDDCS	biopharmaceutics drug disposition classification system
BSEP	bile salt export pump
C	total intracellular concentration of radioactivity in sandwich-cultured hepatocytes
CLapp,met	apparent metabolic clearance
CLh	hepatic plasma clearance
CLh,int,*in vitro*	hepatic intrinsic clearance predicted from *in vitro* assays
CLh,org,*in vitro*	hepatic organ clearance predicted from *in vitro* assays
CLh,org,*in vivo*	hepatic organ clearance based on blood concentrations
CLmet	metabolic clearance
CLren	renal clearance
CLsandwich	transcellular hepatobiliary clearance
CLtot	total organ plasma clearance
DDI	drug-drug interaction
Er	urinary excretion ratio
fu(hep)	unbound fraction in hepatocytes
fu(mic)	unbound fraction in liver microsomes
fu,b	unbound fraction in blood
fu,p	unbound fraction in plasma
IVIVE	*in vitro-in vivo* extrapolation
kgbw	kilogram body weight

KHB	Krebs-Henseleit buffer
Km,bile	affinity constant for the biliary excretion
Km,efflux	affinity constant for the active sinusoidal efflux
Km,met	metabolic affinity constant
Km,uptake	affinity constant for the active uptake
LC-MS	liquid chromatography coupled with mass spectrometry
logD	distribution coefficient
LOQ	limit of quantification
LSC	liquid scintillation counting
MDR/Mdr	multi-drug resistance protein
mRNA	messenger ribonucleic acid
MRP/Mrp	multi-drug resistance associated protein
N.A.	not applicable
N.D.	not determined
OATP/Oatp	organic anion transporting polypeptide
PBPK	physiologically based pharmacokinetics
PSapp,bile	apparent biliary clearance
PSbile	biliary clearance
PSefflux,active	apparent sinusoidal active efflux clearance
PSefflux,passive	sinusoidal passive efflux clearance
PSefflux,total	apparent sinusoidal total efflux clearance
PSuptake,active	apparent active uptake clearance
PSuptake,passive	non-specific passive diffusion
PSuptake,total	total apparent uptake clearance
Qh	rat hepatic blood flow rate
R	compound amount in bile pocket
radio-HPLC	high performance liquid chromatography coupled with on-line radio detection
Rb	blood-to-plasma concentration ratio
S	nominal incubation concentration in buffer system
t	incubation time
Vapp,met	apparent metabolic velocity
Vc	rat hepatocyte volume
Vmax,bile	maximum velocity for the biliary excretion
Vmax,efflux	maximum velocity for the active sinusoidal efflux
Vmax,met	maximum metabolic velocity
Vmax,uptake	maximum velocity for the active sinusoidal uptake
Vuptake,total	total apparent uptake velocity

INTRODUCTION

Predicting the *in vivo* pharmacokinetic characteristics of new chemical entities from *in vitro* studies plays an important role in the modern drug discovery and development processes. This prediction provides essential information for the assessment of drug-drug interactions (DDI), time-dependent pharmacological effects and/or toxic events. Specifically, the liver is the major organ of importance to determine drug disposition in the body. Once compounds reach the liver via the systemic circulation, hepatic elimination starts with the penetration of the drugs through the sinusoidal membrane, followed by metabolism and/or biliary excretion (1). Currently, mainly single pathway analysis methods (e.g. only focusing on the metabolism or hepatic uptake) or methods combining metabolism and transport data in one single system (e.g. sandwich-cultured hepatocytes) are applied to predict *in vivo* hepatic clearances from *in vitro* data (2,3). However, these methods provide often poor correlations between predicted and observed clearances, and are rarely demonstrating a 1 to 1 correlation (4,5). Recently, improved *in vitro-in vivo* extrapolation (IVIVE) was reported using uptake data from primary hepatocytes in a series of different statins (pravastatin, pitavastatin, atorvastatin and fluvastatin) (6). These statins are well-known proto-typical substrates for the organic anion transporting polypeptide (OATP) family, which is responsible for their rate-limiting carrier-mediated hepatic uptake. Unfortunately, hepatic clearances of a more diverse data set cannot be accurately predicted by taking into consideration hepatic uptake data only as other processes may also become rate limiting. Besides metabolism and hepatic influx information, active efflux processes from the inside of hepatocytes must be taken into account (7).

Considering this factor, we propose a novel IVIVE method for predicting rat hepatic clearances using various *in vitro* methods. The following *in vitro* methods were selected from literature: suspended hepatocytes for evaluation of the hepatic uptake clearance, liver microsomes for assessment of metabolic clearance values, and sandwich-cultured hepatocytes for the determination of biliary clearances. The sinusoidal efflux clearance was calculated by combining data obtained from hepatocytes and microsomes. Individual *in vitro* clearance values were substituted into the well-stirred model equation to obtain organ clearance estimations (8,9). A selection of 13 compounds (propranolol, quinidine, verapamil, cyclosporine A, ketoconazole, atorvastatin, aliskiren, pravastatin, valsartan, benzylpenicillin, digoxin, furosemide and ciprofloxacin) with various physicochemical and pharmacokinetic properties, and different class assignments according to the biopharmaceutics drug disposition classification system (BDDCS) was used for these studies (10).

In summary, the goal of our IVIVE analysis method was to develop a prediction method for hepatic organ clearance in rat which considers: 1) All underlying processes as determinants of hepatic elimination (metabolism, transporter-mediated uptake and efflux); 2) A selection of appropriate *in vitro* assays; and 3) A series of physicochemically diverse compounds.

MATERIALS AND METHODS

Materials

[^{3}H]Propranolol (695.6 GBq/mmol), [^{3}H]verapamil (2.59 TBq/mmol), and [^{3}H]digoxin (1.48 TBq/mmol) were purchased from PerkinElmer Life and Analytical Science, Inc. (Boston, MA). [^{3}H]Quindine (740.0 GBq/mmol), [^{3}H] ketoconazole (370.0 GBq/mmol), [^{3}H]atorvastatin (370.0 GBq/mmol), [^{3}H]benzylpenicillin (740.0 GBq/mmol), and [^{3}H]pravastatin (185.0 GBq/mmol) were obtained from American Radiolabeled Chemicals, Inc. (St. Louis, MO). [^{3}H]Cyclosporine A (259.0 GBq/mmol) and [^{14}C]ciprofloxacin (555.0 MBq/mmol) were from GE Healthcare UK Limited (Buckinghamshire UK) and Moravek Biochemicals, Inc. (Brea, CA), respectively. [^{3}H] Valsartan (7.84 GBq/mmol), [^{14}C]aliskiren (2.01 GBq/mmol), and [^{14}C]furosemide (2.14 GBq/mmol) were synthesized in the Isotope Laboratories, Drug Metabolism and Pharmacokinetics, Novartis Pharma AG (Basel, Switzerland). Valsartan and aliskiren were chemically synthesized at Novartis Pharma AG. All the other chemicals and reagents were of analytical grade and purchased from commercial sources.

Uptake Clearance Determination Using Rat Hepatocytes

Cryopreserved pooled rat hepatocytes (pool of 8 male Sprague–Dawley rats, Batch No. Rs573) from Invitrogen Limited (Paisley UK) were used throughout the study. The hepatocytes (viability: 70–85%) were suspended by using Hepatocyte One Step Purification Kit (BD Biosciences; San Jose, CA), and finally adjusted to 2.0×10^6 viable cells/mL by Krebs-Henseleit buffer (KHB). Prior to incubation, the cell suspensions were kept at 37°C or 4°C for 5 min. The incubation was initiated by adding KHB buffer containing the radiolabeled test substances at five different increasing concentrations (final concentrations: 1, 3, 10, 30 and 100 μM, except for cyclosporine A: 0.1, 0.3, 1, 3 and 10 μM) to the cell suspension. After the incubation at 37°C or 4°C for 3 min, the reaction was terminated by separating cells from the substrate solution by the oil extraction method as described in literature (6). Finally, the radioactivity in the medium and within the cells was measured by liquid scintillation counting (LSC; Tricarb-2700TR; PerkinElmer Life Science Products, Inc.).

The total apparent (measured or observed) uptake clearance PSuptake,total (μL/min/10^6 cells) at each substrate concentration S was calculated as the total apparent uptake velocity Vuptake,total (pmol/min/10^6 cells) divided by S (μM). PSuptake,total consists of a saturable (the apparent active uptake clearance PSuptake,active) and a parallel non-saturable (the non-specific passive diffusion PSuptake,passive) component as follows (11):

$$\begin{aligned}\mathrm{PSuptake,total} &= \mathrm{PSuptake,active} + \mathrm{PSuptake,passive}\\ &= \frac{\mathrm{Vmax,uptake}}{\mathrm{Km,uptake}+\mathrm{S}} + \mathrm{PSuptake,passive} \quad (1)\end{aligned}$$

where Vmax,uptake and Km,uptake represent the maximum velocity and the affinity constant for active sinusoidal uptake, respectively.

Unspecific binding events to the assay device and/or the hepatocyte surface will ultimately lead to under- and/or overestimation of the apparent uptake clearance. To account for the loss of compound due to binding events to plastic, control incubations using the same incubation conditions and concentrations in the absence of cellular material were performed. For correction, the apparent uptake clearance values were multiplied by the radioactive recovery ratios from these control experiments. Unspecific binding effects to hepatocytes were identified by parallel incubations at 4°C (same 5 concentrations as used in main experiment) where transporter activity is assumed to be turned off. A potential non-linearity at 4°C is ultimately indicative for an initial concentration loss to the cell system that likely results from unspecific binding events. To quantify the resulting overestimation, assuming binding at the two temperatures to be consistent, the apparent uptake clearance data at 37°C for each substrate concentration S were corrected as follows:

$$\begin{aligned}\mathrm{PSuptake,total} = {} & \mathrm{PSuptake,total}(37^\circ\mathrm{C}) \quad (2)\\ & -((\mathrm{PSuptake,total}(4^\circ\mathrm{C})\\ & -\mathrm{PSuptake,passive}(4^\circ\mathrm{C}))\end{aligned}$$

Determination of the Metabolic Clearance in Rat Microsomes

A reaction mixture of compound at increasing 6–8 different concentrations (0.05–250 μM) in 50 or 100 mM phosphate buffer containing 5 mM $MgCl_2$ (pH 7.4) and NADPH (1 mM) was incubated with pooled liver microsomes (pool of 94 Sprague–Dawley rats, Batch No. 14035, 11271 and 85157; BD Biosciences) at 37°C. The assay was designed to ensure that less than 20% of the initial substrate was consumed at the end of the incubation. The incubation was terminated after 45 min maximum by adding acetonitrile or 5% formic acid in distilled water. Next, all the major metabolite and/or parent compound concentrations in the assay solution were determined by high performance liquid chromatography coupled with on-line radio activity monitoring (radio-HPLC) or mass spectrometry (LC-MS).

For the radio-HPLC analysis, the peak areas of the major metabolites were analyzed using an Agilent Chemstation 1100 HPLC system (Agilent Technologies; Palo Alto, CA) equipped with an HPLC radioactivity detector Flow Star LB513 (Berthold Technologies GmbH; Regensdorf, Switzerland). For the LC-MS analysis (only for benzylpenicillin), the peak area of the parent drug and its internal standard (warfarin) were analyzed using an Agilent Chemstation 1100 HPLC system (Agilent Technologies) equipped with a capillary pump and a triple quadrupole Quattro Ultima mass spectrometer (Waters; Milford, MA). The measurement was operated in a multiple reaction monitoring mode by setting appropriate ion mode with cone voltage and collision energy.

The mobile phase consisted of water, acetonitrile, and formic acid under gradient conditions at a flow rate of 0.25–1.0 mL/min for the radio-HPLC analysis and 60 μL/min for the LC-MS. Peak separation was achieved using Nucleodur Pyramid C18 (125×2 mm, 5 μm, Macherey-Nagel, Düren, Germany), Zorbax SB-C18 (150×4.6 mm, 3.5 μm, Agilent Technologies), Poroshell 300SB-C18 (70×2.1 mm, 5 μm, Agilent Technologies), Synergi 4u MAX-RP (50×1.0 mm, 4.0 μm, Phenomenex; Torrance, CA) or Luna Phenyl-Hexyl (50×1.0 mm, 3.0 μm, Phenomenex) columns.

The apparent metabolic velocity Vapp,met (pmol/min/mg protein) was calculated as the linear increase in the concentration *vs* time plot for the formation of major metabolites except for benzylpenicillin where the linear decrease of parent compound over time was evaluated. The corresponding apparent *in vitro* metabolic clearance CLapp,met (μL/min/mg protein) was obtained by dividing Vapp,met values by the compound concentrations S. For the IVIVE analysis, the microsomal metabolic clearance CLmet (μL/min/mg protein) was calculated, considering a correction for the fraction unbound to liver microsomes fu(mic), as follows (6,12):

$$\mathrm{CLmet} = \frac{\mathrm{CLapp,met}}{\mathrm{fu(mic)}} = \frac{\mathrm{V\,max,met}}{\mathrm{fu(mic)} \cdot (\mathrm{Km,met} + \mathrm{S})} \tag{3}$$

where Vmax,met and Km,met represent the maximum metabolic velocity and metabolic affinity constant, respectively.

Hepatobiliary Disposition in Rat Sandwich-Cultured Hepatocytes

Rat sandwich-cultured hepatocytes (Batch numbers: R-22MAR10-01, R-12APR10-01 R-26APR10-01, R-07JUN10-02, and R-02JUL10-02) were purchased as B-CLEAR®-RT KIT from Qualyst, Inc. (Durham, NC). The hepatobiliary disposition was assessed as previously described in literature (13). Prior to incubation, the hepatocytes were washed with Qualyst (+) Buffer (standard buffer) or Qualyst (−) Buffer (calcium-free buffer). Thereafter, the cells were incubated for 10 min at 37°C with a compound solution in standard buffer at five different increasing concentrations (final concentrations: 1, 3, 10, 30 and 100 μM except for cyclosporine A: 0.1, 0.3, 1, 3 and 10 μM). After washing with ice-cold standard buffer, the cells were solubilized and radioactivity was measured by LSC. The remaining cell lysate was used to determine the protein concentration according to the method of Lowry (Bio-Rad *DC* Protein assay; Bio-Rad Laboratories, Hercules, CA), with bovine serum albumin as a standard.

The apparent biliary clearance PSapp,bile (μL/min/mg protein) was calculated as follows (13):

$$\mathrm{PSapp,bile} = \frac{\mathrm{R}}{\mathrm{A/Vc}}/\mathrm{t} \tag{4}$$

where Vc, A and t represent the average rat hepatocyte volume (5.2 μL/mg protein) (14), the intracellular total radioactivity (μmol/mg protein), and the incubation time (min), respectively. The total compound accumulation in the bile pocket R (pmol/mg protein) was calculated as the difference of the radioactivity in the standard buffer and of the radioactivity in calcium-free buffer after incubation.

Due to metabolism, the intracellular total radioactivity A is likely an overestimation of the effective amount driving biliary clearance, which may result in an underestimation of PSapp,bile (Eq. 4). Consequently, using an analytical method (LSC counting) not allowing determination of intracellular concentrations of unchanged compound, the intracellular total radioactivity A has to be adjusted to account for this underestimation. Applying Michaelis-Menten type kinetics metabolic clearance can be expressed as Vmax,met/(Km,met+S) (see Eq. 3). The metabolic clearance under saturated conditions, where S >> Km,met, is calculated as Vmax,met/S. It is evident that the difference between saturated and non-saturated conditions represents a concentration-dependent measure for the intracellular metabolism and ultimately for the underestimation of PSapp,bile due to metabolism. Consequently, assuming metabolism in sandwich-cultured hepatocytes to be the same as determined in microsomes, for each total intracellular compound concentration C (= A/Vc) a correction factor (so-called *metabolism factor*) can be determined as follows:

$$\begin{aligned}\mathrm{metabolism} \cdot \mathrm{factor} &= \frac{\mathrm{V\,max,met/C}}{\mathrm{V\,max,met/(Km,met + C)}} \\ &= \frac{\mathrm{Km,met + C}}{\mathrm{C}}\end{aligned} \tag{5}$$

With Km,met << C the metabolism factor approaches 1. For all other conditions the metabolism factor is >1. Consequently,

for our IVIVE analysis the biliary clearance PSbile (μL/min/mg protein) was assessed, considering a correction for the fraction unbound in hepatocytes fu(hep), as follows:

$$\mathrm{PSbile} = \frac{\mathrm{PSapp,bile}}{\mathrm{fu(hep)}} = \frac{\mathrm{Vmax,bile}}{\mathrm{fu(hep)} \cdot (\mathrm{Km,bile} + \mathrm{C/metabolism} \cdot \mathrm{factor})} \quad (6)$$

where Vmax,bile and Km,bile represent the maximum velocity and the affinity constant for active biliary excretion, respectively.

The overall apparent hepatobiliary clearance in sandwich-cultured hepatocytes CLsandwich (μL/min/mg protein) for every initial incubation concentration S was calculated by dividing R with S and the incubation time t as described in literature (13).

Assessment of Fraction Unbound in Liver Microsomes and Hepatocytes

fu(mic) values were determined experimentally. Shortly, test substance (final concentration: 0.1 and 1.0 μM) was incubated with pooled liver microsomes in 50 mM phosphate buffer for 10 min at 37°C. The reaction mixture was subjected to ultracentrifugation (L-70 or XL-80 Ultracentrifuge with a rotor of 50.4Ti; Beckman Coulter International S.A., Brea, CA) at 20,989*g* for 3.5 h at 37°C. The fu(mic) value was calculated as the recovery ratio of the radioactivity in microsomes and supernatant as previously described (6). To account for the possible concentration dependency of fu (mic), data analysis according to Scatchard was used (15).

Intracellular binding in hepatoctes was determined as previously reported (16). Assuming concentration-independency, fu(hep) values were derived from distribution coefficients at physiological pH (logD values in Table VI) and the regression equation $\log\mathrm{fu(hep)} = 0.9161 - 0.2567 \cdot \log\mathrm{D}$.

Estimation of the Sinusoidal Efflux Clearance

The apparent sinusoidal total efflux clearance from the intracellular side of hepatocytes back into blood (PSefflux, total) consists of a saturable (the apparent sinusoidal active efflux clearance PSefflux,active) and a parallel non-saturable (the non-specific sinusoidal passive diffusion PSefflux,passive) component as follows:

$$\mathrm{PSefflux,total} = \mathrm{PSefflux,active} + \mathrm{PSefflux,passive} = \frac{\mathrm{Vmax,efflux}}{\mathrm{Km,efflux} + \mathrm{C}} + \mathrm{PSefflux,passive} \quad (7)$$

where Vmax,efflux and Km,efflux represent the maximum velocity and the affinity constant for active sinusoidal efflux, respectively.

PSefflux,total was calculated based on Eq. 8 using CLsandwich data for five incubation concentrations S (1, 3, 10, 30 and 100 μM except for cyclosporine A: 0.1, 0.3, 1, 3 and 10 μM) as an estimate for the overall hepatobiliary clearance in the *in vitro* sandwich-culture hepatocyte system (CLh,int,*in vitro*=CLsandwich). This was done by plugging in the previously determined PSuptake,total parameters from suspended hepatocytes, CLmet from liver microsomes and the PSbile from sandwich-cultured hepatocytes. PSuptake, total data (Eq. 1) refer to the same five incubation concentrations S as described above, whereas PSbile numbers (Eq. 6) refer to the corresponding total intracellular compound concentrations C. Consequently, also CLmet data have to refer to the intracellular drug concentration C. Therefore, with help of Vmax,met, Km, met and fu(mic) (see Table II) the metabolic clearances for every concentration C were calculated using Eq. 3. Evidently, the underlying assumption for this approach is that metabolism and hepatic uptake in sandwich-cultured hepatocytes are the same as determined in microsomes and primary hepatocytes, respectively. Before PSefflux,total estimation, all parameters required to feed into Eq. 8 were converted to a kgbw-basis to account for differences in the diverse assay systems. The following scaling factors derived from literature were applied: 109 [10^6 cells/g liver] for suspended hepatocytes, 54 [mg protein/g liver] for liver microsomes, 111 [mg protein/g liver] for sandwich-cultured hepatocytes, and 40 [g liver/kgbw] for liver weight (13,17).

Prediction of Rat Hepatic Clearances from *In Vitro* Assays

The intrinsic clearance values for hepatic uptake (PSuptake, total at S << Km,uptake), metabolism (CLmet at S << Km,met), biliary excretion (PSbile at C << Km,bile) and sinusoidal efflux (PSefflux,total at C << Km,efflux) were obtained by non-linear curve-fitting according to Eqs. 1, 3, 6 and 7, respectively. With help of these intrinsic clearance values for each individual elimination process the overall (intrinsic) hepatic clearance (CLh,int,*in vitro*) was determined as follows (9):

$$\mathrm{CLh,int,invitro} = \mathrm{PSuptake,total} \cdot \frac{\mathrm{CLmet} + \mathrm{PSbile}}{\mathrm{PSefflux,total} + \mathrm{CLmet} + \mathrm{PSbile}} \quad (8)$$

Finally, the intrinsic hepatic clearances were fed into the well-stirred equation for hepatic organ clearance (CLh,org, *in vitro*) prediction as follows:

$$\mathrm{CLh,org,invitro} = \frac{\mathrm{Qh} \times \mathrm{fu,b} \cdot \mathrm{CLh,int,invitro}}{\mathrm{Qh} + \mathrm{fu,b} \cdot \mathrm{CLh,int,invitro}} \quad (9)$$

where fu,b is the unbound fraction in blood, and Qh is rat hepatic blood flow rate of 50.5 mL/min/kgbw (18).

Data Analysis

All data presented in this study are averages of triplicate determinations. The limit of quantification (LOQ) was taken as the lowest measurement from the radioactive scale which is statistically seen significantly higher than the measured blank value, and for which the standard error of the measurement is lower than 20%. Under the conditions of this study, the LOQ of absolute radioactivity was 20 dpm for ^{14}C-labeled compounds and 60 dpm for ^{3}H-labeled substances.

All concentration-dependent saturation kinetics, assessed *in vitro* as described above, for hepatic uptake (PSuptake,active), oxidative metabolism (CLmet), biliary clearance (PSbile), sinusoidal efflux (PSefflux,active) and overall hepatobiliary clearance (CLsandwich) were fitted according to Michaelis-Menten (compare Eqs. 1, 3, 6 and 7) to obtain the corresponding affinities (Km,uptake, Km, met, Km,bile and Km,efflux) as well as capacity constants (Vmax,uptake, Vmax,met, Vmax,bile, and Vmax,efflux) (12). To obtain estimates for the kinetic parameters data were fitted by a nonlinear least-square method using WinNonlin Ver. 5.2. (Pharsight, Mountain View, CA) and the Enyzme Kinetics Module for SigmaPlot 2004 Version 9.01 (Systat Software Inc., San Jose, CA) for transport and metabolism data, respectively. All other linear regression analyses were performed by Microsoft EXCEL 2007 Version SP3.

In Vivo Pharmacokinetic Parameters

Key pharmacokinetic parameters in rat for all compounds were collected from literature and were partially, when necessary, completed with internal in-house data (Table VI). The fraction unbound in plasma (fu,p) and the blood-to-plasma concentration ratio (Rb) were used for the calculation of fu,b as follows:

$$\mathrm{fu,b} = \frac{\mathrm{fu,p}}{\mathrm{Rb}} \tag{10}$$

Hepatic plasma clearance CLh was generally calculated from the total plasma clearance CLtot by subtraction of the renal plasma clearance CLren (4). The corresponding hepatic organ clearances based on *in vivo* blood concentrations (CLh,org,*in vivo*), which are used for the subsequent IVIVE analysis, were obtained as follows:

$$\mathrm{CLh,org,invivo} = \frac{\mathrm{CLh}}{\mathrm{Rb}} \tag{11}$$

RESULTS

Uptake into Suspended Hepatocytes

The concentration-dependent sinusoidal uptake into rat suspended hepatocytes was investigated for all 13 compounds. The derived Km,uptake, Vmax,uptake, PSuptake,passive as well as the intrinsic (at S << Km,uptake) PSuptake,active and PSuptake,total values according to Eq. 1 are summarized in Table I. Unspecific binding events to the assay system were only observed for the highly lipohilic compounds (radioactive recoveries of 55.6%, 50.0% and 31.3% for propanolol, ketoconazole and cyclosporine A, respectively).

The total influx clearance into suspended hepatocytes was strongly affected by active transporter-mediated uptake processes for all class 3 and 4 compounds, which is consistent with the BDDCS proposed by Wu and Benet (10). For these classes, the PSuptake,total (intrinsic)/PSuptake,passive ratio varied from 1.7 (furosemide) to 16.5 (valsartan), and the non-specific passive diffusion component (PSuptake,passive≤15.8 μL/min/10^6 cells) was generally lower than the contribution of active uptake (7.7≤ intrinsic PSuptake,active≤172.4 μL/min/10^6 cells) to overall clearance. In contrast, the cellular uptake for most class 1 and 2 compounds was mainly governed by a high passive diffusion component (19.1≤PSuptake,passive≤444.7 μL/min/10^6 cells), indicating the active cellular uptake in these classes was likely not to become the rate limiting step for overall organ clearance.

Metabolism in Liver Microsomes

Concentration-dependency of the metabolic velocity was investigated in rat liver microsomal incubations to determine the metabolic clearance of the 12 compounds except for propranolol where the corresponding data were taken from Li *et al.* (19) Together with the corresponding fu(mic), Km,met and Vmax,met data, the intrinsic (at S << Km, met) CLapp,met and CLmet values according to Eq. 3 are summarized in Table II.

All class 1 and 2 compounds (except for cyclosporine A) demonstrated extensive metabolism with larger intrinsic CLmet values. These values ranged from 73.3 μL/min/mg protein (atorvastatin) to 101694.9 μL/min/mg protein (propranolol), which was consistent with the BDDCS. Significantly smaller metabolic clearances have been observed for class 3 and 4 compounds (≤26.1 μL/min/mg protein).

Excretion in Sandwich-Cultured Hepatocyte

Hepatobiliary disposition was determined in rat sandwich-cultured hepatocytes. Intrinisic (at C << Km,bile) PSapp, bile and PSbile parameters, intrinsic CLsandwhich (at very

Table I Kinetic Parameters for the Uptake into Suspended Hepatocytes

Compounds	BDDCS	Km,uptake [μM]	Vmax,uptake [pmol/min/10^6 cells]	PSuptake,passive [μL/min/10^6 cells]	Intrinsic PSuptake,active [μL/min/10^6 cells]	Intrinsic PSuptake,total [μL/min/10^6 cells]
Propranolol	Class 1	0.7 ± 0.7	218.7 ± 90.6	103.2 ± 6.3	321.6 ± 365.7	424.8
Quinidine	Class 1	5.0 ± 2.4	864.9 ± 300.7	32.7 ± 5.9	172.6 ± 100.8	205.3
Verapamil	Class 1	N.A.	N.A.	78.1 ± 1.6	0.0 ± 0.0	78.1
Cyclosporine A	Class 2	N.A.	N.A.	19.1 ± 2.0	43.9 [a] ± 4.2	63.0
Ketoconazole	Class 2	N.A.	N.A.	444.7 ± 54.5	0.0 ± 0.0	444.7
Atorvastatin	Class 2	0.8 ± 0.3	538.6 ± 75.0	48.8 ± 3.2	673.2 ± 277.2	722.1
Aliskiren	Class 3	1.2 ± 0.9	23.5 ± 9.5	14.6 ± 0.6	19.9 ± 17.2	34.6
Pravastatin	Class 3	74.5 ± 12.2	3166.0 ± 478.0	13.1 ± 1.0	42.5 ± 9.5	55.7
Valsartan	Class 3	2.6 ± 0.7	441.4 ± 69.9	11.1 ± 1.6	172.4 ± 55.1	183.5
Benzylpenicillin	Class 3	146.7 ± 25.3	1497.3 ± 239.9	4.7 ± 0.2	10.2 ± 2.4	14.9
Digoxin	Class 4	15.1 ± 5.6	204.9 ± 61.1	3.8 ± 0.5	13.6 ± 6.4	17.4
Furosemide	Class 4	12.2 ± 14.5	138.6 ± 165.2	15.8 ± 2.5	11.3 ± 19.1	27.1
Ciprofloxacin	Class 4	N.A.	N.A.	5.1 ± 0.5	7.7 [a] ± 0.3	12.8

Unspecific binding-corrected uptake into suspended hepatocytes was assessed at five different concentrations with n = 3/concentration as described in the "Materials and Methods" section. Km,uptake, Vmax,uptake, PSuptake,passive and intrinsic PSuptake,active (at S << Km,uptake) values were obtained by non-linear curve fitting according to Eq. 1. Intrinsic PSuptake,total represents the sum of PSuptake,passive and intrinsic PSuptake,active

[a] Because of lack of enough data points these numbers were estimated from the difference of uptake data at 37° and 4°Celsius

N.A. not applicable

low S) as well as *metabolism factor* data together with the calculated fu(hep), Km,bile and Vmax,bile values according to Eqs. 5 and 6 are given in Table III.

Independent of any BDDCS class assignment, the intrinsic biliary clearance component for well-known efflux transporter substrates (quinidine, verapamil, ketoconazole,

Table II Kinetic Parameters for the Metabolism in Liver Microsomes

Compounds	Km,met [μM]	Vmax,met [pmol/min/mg protein]	fu(mic)	Intrinsic CLapp,met [μL/min/mg protein]	Intrinsic CLmet [μL/min/mg protein]
Propranolol	30.0 [a]	1500000 [a]	0.59	50000	101694.9
Quinidine	0.72 ± 0.3	719.1 ± 78.9	0.64	998.8 ± 454.5	1560.6
Verapamil	7.6 ± 5.7	4638.5 ± 1677.4	0.50	610.3 ± 508.2	1220.7
Cyclosporine A	0.46 ± 0.19	5.8 ± 0.92	0.73	12.6 ± 5.6	17.3
Ketoconazole	2.2 ± 0.6	809.4 ± 114.7	0.17	367.9 ± 113.1	2164.2
Atorvastatin	5.1 ± 2.3	189.9 ± 29.4	0.51	37.4 ± 17.8	73.3
Aliskiren	89.6 ± 48.8	1472.8 ± 381.3	0.63	16.4 ± 9.9	26.1
Pravastatin	105 ± 62.9	143.2 ± 48.8	0.88	1.37 ± 0.95	1.56
Valsartan	N.D.	N.D.	0.88	0.25 ± 0.03	0.28
Benzylpenicillin	N.D.	N.D.	0.94	4.9 ± 13.4	5.2
Digoxin	N.D.	N.D.	0.86	1.8 ± 0.22	2.1
Furosemide	37.9 ± 14.7	77.5 ± 13.7	0.80	2.0 ± 0.87	2.6
Ciprofloxacin	N.D.	N.D.	0.82	0.1 ± 0.01	0.13

Metabolism in liver microsomes was assessed at 6–8 different concentrations with *n* = 3/concentration as described in "Materials and Methods" section. Km,met and Vmax,met were obtained by non-linear curve fitting according to Eq. 3, and fu(mic) represents the unbound fraction in microsomes at very low concentrations according to Scatchard (15). Intrinsic CLapp,met (at S<<Km,uptake) is the calculated ratio Vmax,met/Km,met or Vapp,met/S at the lowest incubation concentration if Km,met was not available. Intrinsic CLmet is the calculated ratio intrinsic CLapp,met/fu(mic)

[a] Reported data (19)

N.D. "not determined" due to lack of enough data points

Table III Kinetic Parameters for the Biliary Excretion in Sandwich-Cultured Hepatocyte

	Km,bile [μM]	Vmax,bile [pmol/min/mg]	Intrinsic PSapp,bile [μL/min/mg]	fu(hep)	*Metabolism factor*	Intrinsic PSbile [μL/min/mg]	Intrinsic CLsandwich [μL/min/mg]
Propranolol	41.3 ± 18.4	4.0 ± 1.4	0.097 ± 0.08	0.055	1.39	1.77	6.77
Quinidine	96.8 ± 1085.3	5.9 ± 64.4	0.061 ± 0.03	0.056	1.01	1.08	2.43
Verapamil	N.D.	N.D.	0.058 ± 0.02 [a]	0.043	1.16	1.35	1.97
Cyclosporine A	0.17 ± 0.1	0.13 ± 0.0	0.76 ± 0.34	0.017	1.46	45.0	2.95
Ketoconazole	6.86 ± 0.4	0.104 ± 0.0	0.015 ± 0.02	0.016	1.05	0.98	0.75
Atorvastatin	N.D.	N.D.	0.090 ± 0.08 [a]	0.056	1.26	1.60	0.28
Aliskiren	N.D.	N.D.	7.972 ± 1.20 [a]	0.067	44.29	118.68	0.38
Pravastatin	N.D.	N.D.	2.542 ± 0.50 [a]	0.154	18.16	16.54	0.78
Valsartan	N.D.	N.D.	0.110 ± 0.12 [a]	0.234	1.00	0.47	0.17
Benzylpenicillin	64.7 ± 16.7	5.3 ± 1.2	0.082 ± 0.02	0.410	1.00	0.20	0.36
Digoxin	25.0 ± 11.3	5.2 ± 1.5	0.208 ± 0.07	0.073	1.00	2.86	0.90
Furosemide	N.D.	N.D.	2.472 ± 1.87 [a]	0.205	14.54	12.04	0.25
Ciprofloxacin	N.D.	N.D.	0.240 ± 0.15[a]	0.120	1.00	2.01	0.43

Biliary and overall hepatobiliary excretion in sandwich-cultured hepatocytes was assessed at five different concentrations with $n = 3$/concentration as described in the "Materials and Methods" section. Considering the relationship between PSapp,bile and C/*metabolism factor* for each designated medium concentration, Km,bile and Vmax,bile and intrinsic PSapp,bile (at C << Km,bile) values were obtained by non-linear curve fitting according to Eq. 6. Intrinsic CLsandwich values were assessed similarly by non-linear curve fitting applying ordinary Michaelis-Menten kinetics. The *metabolism factor* was calculated with help of Eq. 5 or was defined as 1.0 if Km,met was not available (see Table II). fu(hep) represents the unbound fraction in hepatocytes derived from log D at pH7.4 and the regression equation $\log fu(hep) = 0.9161 - 0.2567 \cdot \log D$ (16). Intrinsic PSbile is the calculated ratio intrinsic PSapp, bile/fu(hep)

[a] Due to lack of concentration-dependency these numbers represent the average of all biliary excretion measurements

N.D. "not determined" due to lack of enough data points

and digoxin) ranged from 0.98 to 2.86 μL/min/mg protein (20,21). The highest active biliary secretion component could be determined for the efflux transporter substrates aliskiren (intrinsic PSbile = 118.68 μL/min/mg protein) and cyclosporine A (intrinsic PSbile = 45.0 μL/min/mg protein). High biliary clearance activity was also observed for the class 3 compound pravastatin (intrinsic PSbile = 16.54 μL/min/mg protein) and the class 4 compound furosemide (intrinsic PSbile = 12.04 μL/min/mg protein). This suggests that these compounds were also transported by ATP Binding Cassette (ABC) transporter systems expressed at the canalicular membrane of rat hepatocytes. This observation is also supported by literature data (22–24).

Estimation of Efflux Clearance

The derived Km,efflux, Vmax,efflux, PSefflux,passive as well as the intrinsic (at C<< Km, efflux) PSefflux,active and PSefflux,total values according to Eq. 7 are summarized in Table IV. Compounds that are well-known substrates for ABC transporters (quinidine, cyclosporine A, aliskiren and digoxin) have been subjected to efflux processes also at the sinusoidal membrane (20–22). This becomes particularly evident after up-scaling to *in vivo* on a kgbw basis as discussed below. As shown in Table V, for all these compounds the up-scaled PSuptake,passive values from the hepatocyte uptake experiment were significantly less than the corresponding up-scaled intrinsic PSefflux,total data from sandwich-cultured hepatocytes. Similarly, other compounds (pravastatin and, most likely, furosemide) that have been shown to be actively secreted at the biliary membrane also exhibited a significant active sinusoidal efflux (23,24).

Hepatic Clearance Predictions

All (intrinsic) *in vitro* clearance data for uptake (PSuptake, passive, PSuptake,total, PSuptake,active), metabolism (CLmet), biliary excretion (PSbile) and sinusoidal efflux (PSefflux,total, PSefflux,passive and PSefflux,active) were scaled up on a kgbw basis. Subsequently, the CLh,int,*in vitro*, CLh,org,*in vitro* and CLh,org,*in vivo* values were calculated according to Eqs. 8, 9, and 11 (Tables V and VI).

The relationship between reported and predicted hepatic organ clearances is illustrated in Fig. 1. Based on metabolism data only (Fig. 1a), *in vivo* hepatic clearance values were clearly under-predicted ($r^2 = 0.687$, intercept = −4.013). Similarly, overall hepatobiliary excretion in sandwich-cultured hepatocytes (Fig. 1c) provided a significant underestimation of *in vivo* hepatic clearance ($r^2 = 0.321$, intercept = 0.254). In contrast, using only hepatic uptake data (Fig. 1b), *in vivo*

Table IV Kinetic Parameters for the Active Sinusoidal Efflux from Hepatocytes

Compounds	Km,efflux [μM]	Vmax,efflux [nmol/min/kg]	PSefflux,passive [mL/min/kg]	Intrinsic PSefflux,active [mL/min/kg]	Intrinsic PSefflux,total [mL/min/kg]
Propranolol	N.A.	N.A.	296.7 ± 23.9	0.0 ± 0.0	296.7
Quinidine	N.A.	N.A.	253.0 ± 16.1	92.2 ± 16.1	345.3
Verapamil	N.A.	N.A.	204.9 ± 42.5	0.0 ± 0.0	204.9
Cyclosporine A	N.A.	N.A.	N.A.	N.A.	4212.7
Ketoconazole	N.A.	N.A.	N.A.	N.A.	1882.3
Atorvastatin	N.A.	N.A.	N.A.	N.A.	78.5
Aliskiren	N.A.	N.A.	N.A.	N.A.	1224.6
Pravastatin	N.A.	N.A.	N.A.	N.A.	261.2
Valsartan	N.A.	N.A.	56.2 ± 12.2	0.0 ± 0.0	56.2
Benzylpenicillin	12.6 ± 0.6	244.0 ± 112.9	21.8 ± 0.6	19.4 ± 9.0	41.1
Digoxin	N.A.	N.A.	N.A.	N.A.	246.8
Furosemide	N.A.	N.A.	N.A.	N.A.	301.2
Ciprofloxacin	N.A.	N.A.	15.8 ± 2.2	0.0 ± 0.0	15.8

Sinusoidal efflux in sandwich-cultured hepatocytes was assessed as described in the "Materials and Methods" section at five different concentrations from CLsandwich values (with $n = 3$/concentration) according to Eq. 8. Km,efflux, Vmax,efflux, PSefflux,passive and intrinsic PSefflux,active (at $C << Km,efflux$) values were obtained by non-linear curve fitting according to Eq. 7. Intrinsic PSefflux,total represents the sum of PSefflux,passive and intrinsic PSefflux,active or, in the absence of enough dependable data points, was assessed as the calculated ratio PSapp,efflux/C at the lowest incubation concentration

N.A. not applicable

hepatic clearance values were significantly over-predicted ($r^2 = 0.600$, intercept = 15.03). Our new IVIVE analysis method considered all hepatic drug elimination processes (uptake, metabolism, biliary excretion and sinusoidal efflux) and revealed an excellent correlation between *in vivo* clearance data obtained from literature and predicted clearance values (Fig. 1d). Linear regression analysis provided an r^2 value of 0.928 with an intercept of −0.604,

Table V Up-scaled and Predicted Hepatic Clearances from *In vitro* Assays

Compounds	Up-scaled *in vitro* (intrinsic) clearances					Predicted clearances		
	Influx		Metabolism	Excretion		Efflux	CLh,int, *in vitro*	CLh,org, *in vitro*
	PSuptake, passive	PSuptake, total	CLmet	PSbile	CLsandwich	PSefflux, total		
Propranolol	449.9	1852.2	219661.0	7.86	30.1	296.7	1849.7	44.1
Quinidine	142.5	895.2	3370.8	4.80	10.8	345.3	812.1	35.7
Verapamil	340.6	340.6	2636.6	5.99	8.8	204.9	316.1	14.8
Cyclosporine A	83.5	274.8	37.4	201.3	13.1	4212.7	14.7	0.7
Ketoconazole	1939.1	1939.1	4674.6	4.35	3.3	1882.3	1382.8	13.7
Atorvastatin	212.8	3148.1	158.3	7.10	1.2	78.5	2134.9	25.8
Aliskiren	63.8	150.8	56.4	526.9	1.7	1224.6	48.6	20.4
Pravastatin	57.3	242.7	3.37	73.4	3.5	261.2	55.2	24.1
Valsartan	48.5	800.2	0.60	2.09	0.8	56.2	36.6	1.9
Benzylpenicillin	20.4	64.9	11.3	0.89	1.6	41.1	14.9	5.1
Digoxin	16.5	75.7	4.5	12.7	4.0	246.8	4.9	2.7
Furosemide	68.7	118.2	5.5	53.5	1.1	301.2	19.4	2.9
Ciprofloxacin	22.1	55.8	0.28	8.92	1.9	15.8	20.6	12.3

All units are given in mL/min/kgbw. Scaling factors were applied as described in the "Materials and Methods" section. CLh,int,*in vitro* and CLh,org,*in vitro* values were predicted according to Eqs. 8 and 9, respectively

Table VI *In vitro* and *In vivo* Pharmacokinetic Parameters

Compounds	pKa [a]	logD	Protein binding			Total clearance		Renal elimination		Hepatic clearance		References
			fu,p	Rb	fu,b	CLtot [mL/min/kgbw]	CLtot/Rb	CLren [mL/min/kgbw]	Er [b]	CLh [mL/min/kgbw]	CLh,org,*in vivo*	
Propranolol	9.45 (Base)	1.340	0.15	0.80	0.19	78.0	97.5	0.31	0.004	40.4	50.5	(44–47)
Quinidine	8.56 (Base)	1.297	0.30	2.00	0.15	101.7	50.9	0.33	0.003	101.4	50.7	(48,49)
Verapamil	8.92 (Base)	1.752	0.06	0.95	0.066	26.0	27.4	5.28	0.203	20.7	21.8	(46,50–52)
Cyclosporine A	N.A. (Neutral)	3.350	0.06	1.28	0.047	2.4	1.8	0.095	0.04	2.3	1.8	(46,53–55)
Ketoconazole	2.94/6.51 (Base)	3.480	0.01	0.70	0.014	14.4	20.6	1.22	0.084	13.2	18.8	(51,56,57)
Atorvastatin	4.46 (Acid)	1.300	0.03	1.30	0.025	32.3	24.9	0.65	0.02	31.7	24.4	(58–60)
Aliskiren [c]	9.20 (Base)	1.000	0.38	0.54	0.70	20.0	37.0	1.00	0.05	14.0	25.9	–
Pravastatin	4.60 (Acid)	−0.400	0.64	0.77	0.84	35.2	45.8	18.3	0.52	16.9	21.9	(23,33,38)
Valsartan [c]	3.90/4.73 (Acid)	−1.110	0.03	0.55 [c]	0.055	4.2	7.7	0.11	0.025	4.1	7.5	(61)
Benzylpenicillin	2.70 (Acid)	−2.060	0.18	0.46	0.38	16.2	35.1	10.8	0.67	5.3	11.6	(15,62)
Digoxin	N.A. (Neutral)	0.850	0.61	1.04	0.59	7.5	7.2	4.3	0.57	3.2	3.1	(45,46,63–65)
Furosemide	3.90/9.90 (Acid)	−0.890	0.13	0.80 [c]	0.16	2.7	3.4	0.94	0.34	1.8	2.3	(66–68)
Ciprofloxacin	6.09/8.62 (Base)	0.025	0.70	0.89	0.79	33.0	37.2	17.8	0.54	15.0	16.9	(51,69,70)

Compilation of *in vitro* and *in vivo* parameters as published in literature. CLh,org,*in vivo* values were calculated according to Eq. 11

[a] Ionization state at physiological pH is given in parenthesis (46,71, EMEA and FDA labels or Japanese interview forms)

[b] Er: Urinary excretion ratio calculated as CLren/CLtot

[c] In-house data

N.A. not applicable

which is close to the line of unity. The CLh,org,*in vitro*/CLh,org,*in vivo* ratio was between 0.26 (valsartan) and 1.30 (furosemide).

DISCUSSION

Our new IVIVE approach was evaluated for prediction of CLh,org,*in vivo* from CLh,int,*in vitro* using suspended rat hepatocytes, microsomes and sandwich-cultured hepatocytes. The compound set studied consisted of 13 compounds with various physicochemical properties covering all four BDDCS classes (10). The rate determining step of class 1 compounds in hepatic elimination is the passive uptake process into hepatocytes. Class 2 compounds are subject to metabolism and biliary excretion and class 3 compounds have a dominant hepatic active uptake process. All processes for hepatic elimination (uptake, metabolism, biliary excretion and sinusoidal efflux) govern the elimination of class 4 compounds. Well-known equations including the well-stirred model for hepatic organ clearance (Eq. 9) and the physiology-based model for overall intrinsic hepatic clearance estimation, which includes transport processes (Eq. 8) were used (8,25).

For the assessment of hepatic influx, primary hepatocytes in suspension or conventional culture represent useful experimental *in vitro* systems (13). A previous study has demonstrated that rat hepatocytes in suspension showed a higher Oatp-mediated uptake of taurocholate as compared to hepatocytes in culture (26). This is in line with higher Oatp1a1 and Oatp1a4 mRNA levels in the cell suspensions, which were shown to be comparable to the ones observed in liver tissues (26–28). Bow *et al.* showed that ABC transporters like the multi-drug resistant protein Mdr1 and the multi-drug resistant associated protein Mrp2 are not accurately sorted to the canalicular membrane of freshly prepared rat hepatocytes. Thus, use of these cells will cause an inaccurate assessment of the biliary excretion (29). Independent of the experimental system used, significant differences in activity have been reported for active hepatic uptake (28). Batch-to-batch variations and inherent genetic variability are considered as the main reasons for these activity differences. For example, the uptake of estradiol 17β-D-glucuronide into various batches of freshly prepared or cryopreserved hepatocytes was reported to be variable. Well-known genetic polymorphisms of OATP family transporters such as OATP1B3 are likely the cause for this observation (30). To account for batch-to-batch variations, only a single batch of pooled cryopreserved hepatocytes in suspension (pool of 8 male rats) was used for the evaluation of sinusoidal uptake in the present study.

For studying oxidative hepatic metabolism, liver microsomes have been proven to be a robust system (31). In

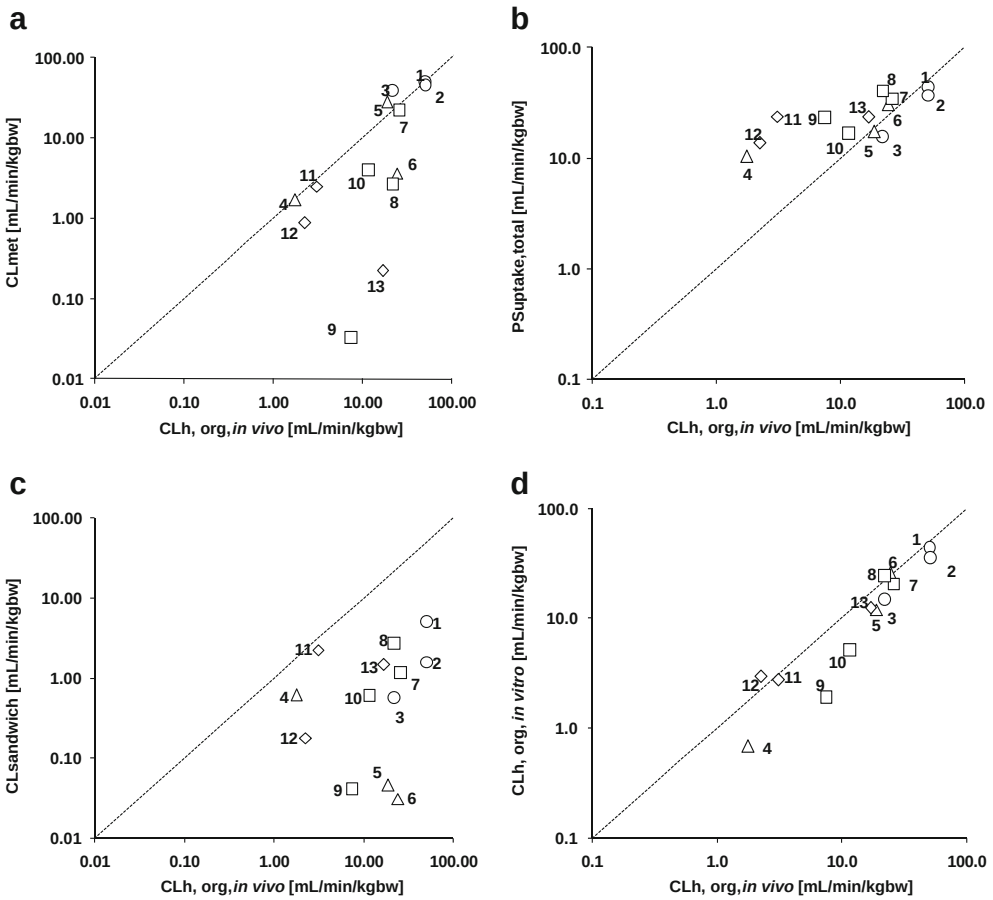

Fig. 1 Comparison of the reported and predicted hepatic clearances in rats as summarized in Tables V and VI. (**a** and **b**) Predicted CLh,org,*in vitro* values from single parameter analysis using intrinsic CLmet and intrinsic PSuptake,total data, respectively. (**c**) Predicted *in vivo* hepatic clearance based on intrinsic CLsandwich results. (**d**) Relationship between CLh,org,*in vitro* and CLh,org,*in vivo* according to the new IVIVE analysis method taking all hepatic clearance pathways into account. Circles, triangles, squares and diamonds show the class 1, 2, 3 and 4 assignments according to BDDCS (10), respectively. The dotted line represents the line of unity. The numbering of drugs is as follows: 1.propranolol; 2. quinidine; 3.verapamil; 4.cyclosporine A; 5.ketoconazole; 6.atorvastatin; 7.aliskiren; 8.pravastatin; 9.valsartan; 10.benzylpenicillin; 11.digoxin; 12.furosemide; 13.ciprofloxacin.

addition to oxidative metabolism, hepatocytes could also be used to determine drug conjugation reactions, such as glucuronidation and sulfation (32,33). However, hepatic uptake transporters are well known to modulate clearance of drugs that are eliminated by overall metabolism in an *in vitro* hepatocyte systems (34). Since contribution of conjugation pathways to overall hepatic elimination was negligible for almost all the selected compounds in the present study, a single batch of pooled liver microsomes (pool of 94 rats) was used for the direct assessment of transporter-independent oxidative metabolism throughout the study.

In contrast to freshly prepared primary hepatocytes, sandwich-cultured hepatocytes retain/regain the intact canalicular networks and polarized excretory function including sinusoidal efflux (13). Many studies have utilized hepatocytes in suspension to examine the efflux of compounds, but this approach does not differentiate between canalicular excretion and sinusoidal efflux (13). The hepatic influx clearances can also be evaluated in sandwich-cultured hepatocytes, although lower mRNA expression levels of uptake transporters were reported as compared to hepatocytes in suspension (26). The sinusoidal uptake of digoxin, pravastatin and rosuvastatin was decreased in long time sandwich-cultured hepatocytes because of the down-regulation of hepatic uptake transporters (35). Despite these limitations, the use of sandwich-cultured hepatocytes was still shown to be a viable approach to estimate the biliary and overall hepatic clearance. This provides a basis for the heterogenic calculation of sinusoidal efflux clearance (Eq. 8). *In vitro* intrinsic biliary clearance values generated in sandwich-cultured hepatocytes were demonstrated to correlate well with *in vivo* biliary clearance data for compounds whose major elimination route is not metabolism (olmesartan, pitavastatin and rosuvastatin) (13). However, due to the lack of bile flow and the down-regulation of uptake and/or biliary transporter levels like OATP, MRP2, bile salt export pump (BSEP) and breast cancer resistance protein (BCRP), sandwich-cultured hepatocytes may have the tendency to underestimate the prediction of biliary clearances by 2.5–20 times (13,35,36). Similarly, strong metabolism and/or strong protein binding might provide underestimations of biliary clearance (37,38). Consequently, the present IVIVE analysis was based on total radioactivity data in sandwich-cultured hepatocytes which included correction factors for the fraction unbound in the hepatocytes (fu(hep)) and for microsomal metabolism (*metabolism factor*) (16). When the fu (hep) was not taken into consideration, the present IVIVE

method has actually resulted in much less accurate predictions (data not shown).

Although the first demonstration of *in vitro-in vivo* prediction was published more than 30 years ago, the common practice is still to use a single parameter of drug metabolism data from microsomes, hepatocytes or liver slices for the prediction of *in vivo* hepatic clearance (39–41). Only recently, the utility of *in vitro* drug transport data such as uptake into fresh or cryopreserved hepatocytes and hepatobiliary excretion in sandwich-cultured hepatocytes has been investigated in order to predict *in vivo* organ clearances (6,13,36). In general, inconsistent and imprecise predictions were obtained for *in vitro* absolute clearance values using such single parameter approaches. Metabolism data from microsomes as well as from hepatocytes often provided underpredictions for hepatic clearance, whereas liver uptake data from hepatocytes tended to overestimate hepatic clearance (42,43). This general observation could be confirmed with the present data set. As shown in Fig. 1a, we found a significant underestimation of *in vivo* hepatic clearance using only microsomal metabolism data. *In vitro* metabolism data are most predictive for the highly cleared class 1 and class 2 compounds where intrinsic metabolism is rate limiting for the overall organ clearance. Most of the basic and neutral compounds in the data set tend to be class 1 or 2 compounds (Table VI). Since class 1 and 2 compounds exhibit a high passive diffusion potential, active cellular uptake is likely not the rate limiting step for overall organ clearance. Consequently, these compounds will easily penetrate the sinusoidal membrane by passive diffusion, and will be subjected to metabolism and/or biliary excretion. In contrast, all acidic compounds in the data set (except atorvastatin) were assigned to BDDCS class 3 or 4 where active uptake, biliary excretion and efflux transport processes are the predominant factors influencing overall hepatic clearance (Tables I, III and IV). Neglecting the biliary excretion process for class 4 compounds will inevitably result in an underestimation of hepatic clearance, which is confirmed by literature data. Underprediction from *in vitro* metabolism was most prominent for acidic compounds while the prediction was better for basic and neutral compounds (42). In contrast, the single parameter IVIVE analysis using hepatic uptake data only resulted in a significant overestimation of the *in vivo* clearance as previously reported (Fig. 1b). The *in vitro* hepatic uptake data are more predictive for the highly cleared class 1 and 3 compounds, where total cellular uptake is the rate limiting process for overall organ clearance. The observed overestimation is most prominent for compounds with low hepatic extraction ratio (4). Most of these compounds (cyclosporine A, digoxin and furosemide) can clearly be assigned to BDDCS class 2 or 4 where biliary excretion and/or sinusoidal efflux processes are the known major determinants for hepatic elimination (10). Considering Eq. 8 developed by Kusuhara and Sugiyama (8), the overall hepatic clearance is generally less than total hepatic uptake clearance (PSuptake,total) when sinusoidal efflux is not much smaller than the sum of biliary excretion and metabolism. The prerequisite assumption is that the drug equilibration in liver tissue is not the rate-determining process. Consequently, a prediction method considering all the outlined hepatic clearance processes (influx, metabolism, biliary excretion and sinusoidal efflux) is expected to provide better predictions compared to single pathway methods using only influx or metabolism data. However, as illustrated in Fig. 1c overall hepatobiliary clearance data from sandwich-cultured hepatocytes were similarly providing significant underestimations of *in vivo* hepatic clearance as observed in microsomes. Strong metabolism and lack of metabolite excretion into bile are the most prominent reasons for this underestimation. On the other hand, our novel IVIVE method provides a very good correlation (r^2 value was 0.928) between predicted and reported clearances, and demonstrates almost a 1 to 1 correlation with the line of unity as shown in Fig. 1d. The high degree of the correlation was unexpected given the heterogeneity of the data set (inclusion of low and high clearance drugs, physicochemical diversity), and the known limitation of the *in vitro* models applied. A further extension of the present IVIVE method to other compounds which are at least partially subject to Phase II metabolism as e.g. some nonsteroidal anti-inflammatory drugs or 3′-azido-3′-deoxythzmidine (32) will likely diminish the correlation. The hepatic clearance of valsartan was underestimated in the present prediction (Fig. 1d) which is in line with this hypothesis since valsartan is known to be strongly metabolized to an acyl glucuronide (in-house data). Similarly, the tendency of sandwich-cultured hepatocytes to underestimate the prediction of biliary clearance is expected to impact the power of the prediction. The *in vivo* biliary clearance data from seven drugs (ketoconazole, atorvastatin, aliskiren, pravastatin, valsartan, benzylpenicillin and ciprofloxacin) were available and the comparison with the measured *in vitro* PSbile numbers showed a good correlation under the linear regression analysis (r^2 value of 0.790; data not shown). However, the determined *in vitro* biliary clearance was negligible for 9 out of the 13 compounds in the data set, which consequently limited the overall assessment of its role in hepatic clearance prediction. Nevertheless, the presented method using a series well established and easy to perform *in vitro* assays was shown to be useful in the prediction of rat hepatic organ clearance. Future extensions of this research should focus on increasing the number of compounds with different disposition and elimination profiles.

In addition, future research should include assessments of other *in vitro* methods not used in this study to determine their usefulness and applicability to IVIVE while taking into account all known underlying processes of hepatic elimination.

CONCLUSION

The use of *in vitro* systems makes it possible to produce quantitative data on hepatic drug metabolism and transport prior to studying pharmacokinetics *in vivo*. Thus, these systems should be selected carefully and their use should be thoroughly investigated and validated. The present study demonstrates that well-established *in vitro* assays such as microsomes and hepatocytes may be used for obtaining intrinsic hepatic clearance value estimates. Therefore, information on new compounds can readily be placed in the context of existing information.

Considering the absolute clearance processes of hepatic influx, metabolism, biliary excretion and sinusoidal efflux, the rat hepatic clearances of 13 compounds with various physicochemical and pharmacokinetic characteristics were well predicted. In contrast, hepatic clearance estimates from single parameter analysis (metabolism or hepatic uptake) were poorly predictive for the *in vivo* state. Our new IVIVE method provides excellent predictions for our tested set of compounds and it remains to be exploited where its limitations are. Future extensions of this approach will focus on the clearance predictions for human, potential compound assignment strategies according to BDDCS and the early assessment of the DDI potential of new drug candidates. In addition, upcoming research will include robust physiologically-based pharmacokinetic (PBPK) modeling, providing the opportunity of assessing the precise time-dependent pharmacological and toxicological effects of new chemical entities.

ACKNOWLEDGMENTS & DISCLOSURES

The authors wish to acknowledge the many Novartis Drug Metabolism and Pharmacokinetic Department Scientists of Basel Switzerland who have supported generation of data used in these analyses. Special thanks go to Drs. Heike Gutmann, Joel Krauser and Birk Poller for their critical evaluation of this work.

REFERENCES

1. Müller M, Jansen PL. Molecular aspects of hepatobiliary transport. Am J Physiol. 1997;272(6 Pt 1):G1285–303.
2. Lee JK, Marion TL, Abe K, Lim C, Pollock GM, Brouwer KL. Hepatobiliary disposition of troglitazone and metabolites in rat and human sandwich-cultured hepatocytes: use of Monte Carlo simulations to assess the impact of changes in biliary excretion on troglitazone sulfate accumulation. J Pharmacol Exp Ther. 2010;332(1):26–34.
3. Treijtel N, van Eijkeren JC, Nijmeijer S, de Greef-van der Sandt IC, Freidig AP. Clearance and clearance inhibition of the HIV-1 protease inhibitors ritonavir and saquinavir in sandwich-cultured rat hepatocytes and rat microsomes. Toxicol In Vitro. 2009;23(1):185–93.
4. Iwatsubo T, Hirota N, Ooie T, Suzuki H, Shimada N, Chiba K, *et al.* Prediction of *in vivo* drug metabolism in the human liver from *in vitro* metabolism data. Pharmacol Ther. 1997;73(2):147–71.
5. Obach RS. Prediction of human clearance of twenty-nine drugs from hepatic microsomal intrinsic clearance data: An examination of *in vitro* half-life approach and nonspecific binding to microsomes. Drug Metab Dispos. 1999;27(11):1350–9.
6. Watanabe T, Kusuhara H, Maeda K, Kanamaru H, Saito Y, Hu Z, *et al.* Investigation of the rate-determining process in the hepatic elimination of HMG-CoA reductase inhibitors in rats and humans. Drug Metab Dispos. 2010;38(2):215–22.
7. Yamazaki M, Suzuki H, Sugiyama Y. Recent advances in carrier-mediated hepatic uptake and biliary excretion of xenobiotics. Pharm Res. 1996;13(4):497–513.
8. Kusuhara H, Sugiyama Y. Pharmacokinetic modeling of the hepatobiliary transport mediated by cooperation of uptake and efflux transporters. Drug Metab Rev. 2010;42(3):539–50.
9. Kusuhara H, Sugiyama Y. *In vitro-in vivo* extrapolation of transporter-mediated clearance in the liver and kidney. Drug Metab Pharmacokinet. 2009;24(1):37–52.
10. Wu CY, Benet LZ. Predicting drug disposition via application of BCS: transport/absorption/elimination interplay and development of a biopharmaceutics drug disposition classification system. Pharm Res. 2005;22(1):11–23.
11. Hassen AM, Lam D, Chiba M, Tan E, Geng W, Pang KS. Uptake of sulfate conjugates by isolated rat hepatocytes. Drug Metab Dispos. 1996;24(7):792–8.
12. Eadie GS. The inhibition of cholinesterase by physostigmine and prostigmine. J Biol Chem. 1942;146:85–93.
13. Swift B, Pfeifer ND, Brouwer KL. Sandwich-cultured hepatocytes: an *in vitro* model to evaluate hepatobiliary transporter-based drug interactions and hepatotoxicity. Drug Metab Rev. 2010;42(3):446–71.
14. Lee PS, Song IS, Shin TH, Chung SJ, Shim CK, Song S, *et al.* Kinetic analysis about the bidirectional transport of 1-anilino-8-naphthalene sulfonate (ANS) by isolated rat hepatocytes. Arch Pharm Res. 2003;26(4):338–43.
15. Tsuji A, Yoshikawa T, Nishide K, Minami H, Kimura M, Nakashima E, *et al.* Physiologically based pharmacokinetic model for beta-lactam antibiotics I: tissue distribution and elimination in rats. J Pharm Sci. 1983;72(11):1239–52.
16. Yabe Y, Galetin A, Houston JB. Kinetic characterization of rat hepatic uptake of 16 actively transported drugs. Drug Metab Dispos. 2011;39(10):1808–14.
17. Carlile DJ, Zomorodi K, Houston JB. Scaling factors to relate drug metabolic clearance in hepatic microsomes, isolated hepatocytes, and the intact liver: studies with induced livers involving diazepam. Drug Metab Dispos. 1997;25(8):903–11.
18. Pollack GM, Brouwer KL, Demby KB, Jones JA. Determination of hepatic blood flow in the rat using sequential infusions of indocyanine green or galactose. Drug Metab Dispos. 1990;18(2):197–202.
19. Li X, Zeng S. Stereoselective propranolol metabolism in two drug induced rat hepatic microsomes. World J Gastroenterol. 2000;6(1):74–8.
20. Adachi Y, Suzuki H, Sugiyama Y. Comparative studies on *in vitro* methods for evaluating *in vivo* function of MDR1 P-glycoprotein. Pharm Res. 2001;18(12):1660–8.

21. Fan Y, Rodriguez-Proteau R. Ketoconazole and the modulation of multidrug resistance-mediated transport in Caco-2 and MDCKII-MDR1 drug transport models. Xenobiotica. 2008;38 (2):107–29.
22. Vaidyanathan S, Camenisch G, Schuetz H, Reynolds C, Yeh CM, Bizot MN, *et al*. Pharmacokinetics of the oral direct renin inhibitor aliskiren in combination with digoxin, atorvastatin, and ketoconazole in healthy subjects: the role of P-glycoprotein in the disposition of aliskiren. J Clin Pharmacol. 2008;48(11):1323–38.
23. Yamazaki M, Akiyama S, Niinuma K, Nishigaki R, Sugiyama Y. Biliary excretion of pravastatin in rats: contribution of the excretion pathway mediated by canalicular multispecific organic anion transporter. Drug Metab Dispos. 1997;25(10):1123–9.
24. Hasegawa M, Kusuhara H, Adachi M, Schuetz JD, Takeuchi K, Sugiyama Y. Multidrug resistance-associated protein 4 is involved in the urinary excretion of hydrochlorothiazide and furosemide. J Am Soc Nephrol. 2007;18(1):37–45.
25. Wilkinson GR, Shand DG. Commentary: a physiological approach to hepatic drug clearance. Clin Pharmacol Ther. 1975;18 (4):377–90.
26. Jørgensen L, Van Beek J, Lund S, Schousboe A, Badolo L. Evidence of Oatp and Mdr1 in cryopreserved rat hepatocytes. Eur J Pharm Sci. 2007;30(2):181–9.
27. Luttringer O, Theil FP, Lavé T, Wernli-Kuratli K, Guentert TW, de Saizieu A. Influence of isolation procedure, extracellular matrix and dexamethasone on the regulation of membrane transporters gene expression in rat hepatocytes. Biochem Pharmacol. 2002;64(11):1637–50.
28. Shitara Y, Li AP, Kato Y, Lu C, Ito K, Itoh T, *et al*. Function of uptake transporters for taurocholate and estradiol 17beta-D-glucuronide in cryopreserved human hepatocytes. Drug Metab Pharmacokinet. 2003;18(1):33–41.
29. Bow DA, Perry JL, Miller DS, Pritchard JB, Brouwer KL. Localization of P-gp (Abcb1) and Mrp2 (Abcc2) in freshly isolated rat hepatocytes. Drug Metab Dispos. 2008;36(1):198–202.
30. Kalliokoski A, Niemi M. Impact of OATP transporters on pharmacokinetics. Br J Pharmacol. 2009;158(3):693–705.
31. Soars MG, Grime K, Sproston JL, Webborn PJ, Riley RJ. Use of hepatocytes to assess the contribution of hepatic uptake to clearance *in vivo*. Drug Metab Dispos. 2007;35(6):859–65.
32. Mano Y, Usui T, Kamimura H. Comparison of inhibition potentials of drugs against zidovudine glucuronidation in rat hepatocytes and liver microsomes. Drug Metab Dispos. 2007;35(4):602–6.
33. Watanabe T, Kusuhara H, Maeda K, Shitara Y, Sugiyama Y. Physiologically based pharmacokinetic modeling to predict transporter-mediated clearance and distribution of pravastatin in humans. J Pharmacol Exp Ther. 2009;328(2):652–62.
34. Webborn PJ, Parker AJ, Denton RL, Riley RJ. *In vitro-in vivo* extrapolation of hepatic clearance involving active uptake: theoretical and experimental aspects. Xenobiotica. 2007;37(10–11):1090–109.
35. Kotani N, Maeda K, Watanabe T, Hiramatsu M, Gong LK, Bi YA, Takezawa T, Kusuhara H, Sugiyama Y. Culture period-dependent changes in the uptake of transporter substrates in sandwich-cultured rat and human hepatocytes. Drug Metab Dispos. 2011;39(9):1503–10.
36. Li N, Singh P, Mandrell KM, Lai Y. Improved extrapolation of hepatobiliary clearance from *in vitro* sandwich cultured rat hepatocytes through absolute quantification of hepatobiliary transporters. Mol Pharm. 2010;7(3):630–41.
37. Kilford PJ, Gertz M, Houston JB, Galetin A. Hepatocellular binding of drugs: correction for unbound fraction in hepatocyte incubations using microsomal binding or drug lipophilicity data. Drug Metab Dispos. 2008;36(7):1194–7.
38. Sasaki M, Suzuki H, Aoki J, Ito K, Meier PJ, Sugiyama Y. Prediction of *in vivo* biliary clearance from the *in vitro* transcellular transport of organic anions across a double-transfected Madin-Darby canine kidney II monolayer expressing both rat organic anion transporting polypeptide 4 and multidrug resistance associated protein 2. Mol Pharmacol. 2004;66(3):450–9.
39. Rane A, Wilkinson GR, Shand DG. Prediction of hepatic extraction ratio from *in vitro* measurement of intrinsic clearance. J Pharmacol Exp Ther. 1977;200(2):420–4.
40. Wilkinson GR. Clearance approaches in pharmacology. Pharmacol Rev. 1987;39(1):1–47.
41. Olinga P, Hof IH, Merema MT, Smit M, de Jager MH, Swart PJ, *et al*. The applicability of rat and human liver slices to the study of mechanisms of hepatic drug uptake. J Pharmacol Toxicol Methods. 2001;45(1):55–63.
42. Sohlenius-Sternbeck AK, Afzelius L, Prusis P, Neelissen J, Hoogstraate J, Johansson J, *et al*. Evaluation of the human prediction of clearance from hepatocyte and microsome intrinsic clearance for 52 drug compounds. Xenobiotica. 2010;40(9):637–49.
43. Sathirakul K, Suzuki H, Yasuda K, Hanano M, Sugiyama Y. Construction of a physiologically based pharmacokinetic model to describe the hepatobiliary excretion process of ligands: quantitative estimation of intracellular diffusion. Biol Pharm Bull. 1993;16 (3):273–9.
44. Letendre L, Scott M, Dobson G, Hidalgo I, Aungst B. Evaluating barriers to bioavailability *in vivo*: validation of a technique for separately assessing gastrointestinal absorption and hepatic extraction. Pharm Res. 2004;21(8):1457–62.
45. Liu X, Smith BJ, Chen C, Callegari E, Becker SL, Chen X, *et al*. Evaluation of cerebrospinal fluid concentration and plasma free concentration as a surrogate measurement for brain free concentration. Drug Metab Dispos. 2006;34(9):1443–7.
46. Poulin P, Theil FP. Prediction of pharmacokinetics prior to *in vivo* studies. 1. Mechanism-based prediction of volume of distribution. J Pharm Sci. 2002;91(1):129–56.
47. Tomcíková O, Bezek S, Durisová M, Faberová V, Zemánek M, Trnovec T. Biliary excretion and enterohepatic circulation of two beta-adrenergic blocking drugs, exaprolol and propranolol, in rats. Biopharm Drug Dispos. 1984;5(2):153–62.
48. Sugihara N, Furuno K, Kita N, Murakami T, Yata N. Distribution of quinidine in rats with carbon tetrachloride-intoxicated hepatic disease. J Pharmacobiodyn. 1992;15(4):167–74.
49. Watari N, Wakamatsu A, Kaneniwa N. Comparison of disposition parameters of quinidine and quinine in the rat. J Pharmacobiodyn. 1989;12(10):608–15.
50. Bhatti MM, Foster RT. Pharmacokinetics of the enantiomers of verapamil after intravenous and oral administration of racemic verapamil in a rat model. Biopharm Drug Dispos. 1997;18 (5):387–96.
51. Yamano K, Yamamoto K, Kotaki H, Takedomi S, Matsuo H, Sawada Y, *et al*. Correlation between *in vivo* and *in vitro* hepatic uptake of metabolic inhibitors of cytochrome P-450 in rats. Drug Metab Dispos. 1999;27(11):1225–31.
52. Ling S, Jamali F. The effect of infliximab on hepatic cytochrome P450 and pharmacokinetics of verapamil in rats with pre-adjuvant arthritis: a drug-disease and drug-drug interaction. Basic Clin Pharmacol Toxicol. 2009;105(1):24–9.
53. Kawai R, Mathew D, Tanaka C, Rowland M. Physiologically based pharmacokinetics of cyclosporine A: extension to tissue distribution kinetics in rats and scale-up to human. J Pharmacol Exp Ther. 1998;287(2):457–68.
54. Tanaka C, Kawai R, Rowland M. Dose-dependent pharmacokinetics of cyclosporin A in rats: events in tissues. Drug Metab Dispos. 2000;28(5):582–9.
55. Wagner O, Schreier E, Heitz F, Maurer G. Tissue distribution, disposition, and metabolism of cyclosporine in rats. Drug Metab Dispos. 1987;15(3):377–83.

56. Remmel RP, Amoh K, Abdel-Monem MM. The disposition and pharmacokinetics of ketoconazole in the rat. Drug Metab Dispos. 1987;15(6):735–9.
57. Saadeddin A, Peris JE. Pharmacokinetic interaction between efavirenz and ketoconazole in rats. Xenobiotica. 2009;39 (2):135–9.
58. Black AE, Hayes RN, Roth BD, Woo P, Woolf TF. Metabolism and excretion of atorvastatin in rats and dogs. Drug Metab Dispos. 1999;27(8):916–23.
59. Lau YY, Okochi H, Huang Y, Benet LZ. Pharmacokinetics of atorvastatin and its hydroxy metabolites in rats and the effects of concomitant rifampicin single doses: relevance of first-pass effect from hepatic uptake transporters, and intestinal and hepatic metabolism. Drug Metab Dispos. 2006;34(7):1175–81.
60. Paine SW, Parker AJ, Gardiner P, Webborn PJ, Riley RJ. Prediction of the pharmacokinetics of atorvastatin, cerivastatin, and indomethacin using kinetic models applied to isolated rat hepatocytes. Drug Metab Dispos. 2008;36(7):1365–74.
61. Fukuda H, Ohashi R, Tsuda-Tsukimoto M, Tamai I. Effect of plasma protein binding on *in vitro-in vivo* correlation of biliary excretion of drugs evaluated by sandwich-cultured rat hepatocytes. Drug Metab Dispos. 2008;36(7):1275–82.
62. Michel G, Bergeron F, John G, Michael B, Louis W, Stanley C. Renal tubular transport of penicillin G and carbenicillin in the rat. J Infect Dis. 1975;132(4):374–83.
63. Harrison LI, Gibaldi M. Pharmacokinetics of digoxin in the rat. Drug Metab Dispos. 1976;4(1):88–93.
64. Peng SX, Ritchie DM, Cousineau M, Danser E, Dewire R, Floden J. Altered oral bioavailability and pharmacokinetics of P-glycoprotein substrates by coadministration of biochanin A. J Pharm Sci. 2006;95(9):1984–93.
65. Evans RL, Owens SM, Ruch S, Kennedy RH, Seifen E. The effect of age on digoxin pharmacokinetics in Fischer-344 rats. Toxicol Appl Pharmacol. 1990;102(1):61–7.
66. Chen C, Scott D, Hanson E, Franco J, Berryman E, Volberg M, *et al.* Impact of Mrp2 on the biliary excretion and intestinal absorption of furosemide, probenecid, and methotrexate using Eisai hyperbilirubinemic rats. Pharm Res. 2003;20(1):31–7.
67. Wallin JD, Ryals P, Kaplowitz N. Metabolic clearance of furosemide in the rat. J Pharmacol Exp Ther. 1977;200(1):52–7.
68. Yang KH, Choi YH, Lee U, Lee JH, Lee MG. Effects of cytochrome P450 inducers and inhibitors on the pharmacokinetics of intravenous furosemide in rats: involvement of CYP2C11, 2E1, 3A1 and 3A2 in furosemide metabolism. J Pharm Pharmacol. 2009;61(1):47–54.
69. Chen Q, Tung EC, Ciccotto SL, Strauss JR, Ortiga R, Ramsay KA, *et al.* Effect of the anticoagulant ethylenediamine tetra-acetic acid (EDTA) on the estimation of pharmacokinetic parameters: A case study with tigecycline and ciprofloxacin. Xenobiotica. 2008;38(1):76–86.
70. Nouaille-Degorce B, Veau C, Dautrey S, Tod M, Laouari D, Carbon C, *et al.* Influence of renal failure on ciprofloxacin pharmacokinetics in rats. Antimicrob Agents Chemother. 1998;42(2):289–92.
71. Lombardo F, Obach RS, Shalaeva MY, Gao F. Prediction of human volume of distribution values for neutral and basic drugs. 2. Extended data set and leave-class-out statistics. J Med Chem. 2004;47(5):1242–50.